Inside-outside hadronization in a medium

B.Z. Kopeliovich[1,2], J. Nemchik[3], E. Predazzi[4], and A. Hayashigaki[2]

[1] Max-Planck Institut für Kernphysik, Postfach 103980, 69029 Heidelberg, Germany
[2] Institut für Theoretische Physik der Universität, 93040 Regensburg, Germany
[3] Institute of Experimental Physics SAV, Watsonova 47, CS-04353 Kosice, Slovakia
[4] Dipartimento di Fisica Teorica, Università di Torino and INFN, Sezione di Torino,
    I-10125, Torino, Italy

Abstract. Nuclei are unique analyzers for the early stage of the space-time development of hadronization. DIS at medium energies is especially suitable for this task being sensitive to hadronization dynamics, since the production length is comparable with the nuclear size. This was the driving motivation to propose an experiment at HERMES [1], and provide predictions based on a pQCD model of hadronization. Now the experiment is done and one can compare the predictions with data [2]. The model successfully describes with no adjustment the nuclear effects for various energies, z_h, p_T, and Q^2, for different flavors and different nuclei. It turns out that the main source of nuclear suppression of the hadron production rate is attenuation of colorless pre-hadrons in the medium. An alternative model [11] is based upon an unjustified assumption that the struck parton keeps radiating gluons far beyond the nuclear size and the pre-hadron is produced outside the nucleus. This model has apparent problems attempting to explain certain features of the results from HERMES. A good understanding of the hadronization dynamics is important for proper interpretation of the strong suppression of high-p_T hadrons observed in heavy ion collisions at RHIC. We demonstrate that the production length is even shorter in this case and keeps contracting with rising p_T.

PACS. 24.85.+p Quarks, gluons, and QCD in nuclei and nuclear processes – 25.30.Rw Electroproduction reactions – 25.75.Dw Particle and resonance production

1 Introduction

Recent measurements of inclusive production of hadrons in deep-inelastic scattering (DIS) off nuclei by the HERMES collaboration [2] have provided precious information about the space-time development of hadronization. These measurements were proposed [1] back in 1995 and predictions were made within a model of hadronization based on perturbative QCD. One of the goals was to reach a better understanding of in-medium hadronization in order to provide a more reliable interpretation of high-p_T hadron production in heavy ion collisions considered as a probe for a created dense matter.

Now, when some of the results of these measurements are released, it is proper to compare the predictions with the data and draw conclusions. In present paper we revisit the problem of in-medium hadronization, re-introduce the model, and perform calculations in accordance with the concrete kinematics of HERMES data. We demonstrate that absorption of the produced colorless pre-hadron is the main source of nuclear suppression. Our predictions need no adjustment and are in a good agreement with data.

Older models [3,4,5,6,7] were based on the string model which were quite pedagogical and helpful for intuitive understanding of the space-time development of hadronization. On the other hand, one could not consider such a nonperturbative phenomenology as a realistic scheme for hard reactions like DIS. These models had a very low predictive power, no access to Q^2 and p_T-dependences, missed the effect of color transparency, etc.

The release of data from the HERMES experiment has stimulated a new wave of theoretical models. All of them have low predictive power and are simply fitted to data which are supposed to be explained. This is why all of them agree with data, although they explore quite different physical ideas.

Some of the models [8,9,10] continue developing already known ideas based on the phenomenology of nonperturbative hadronization. Others [11,12], employ the idea of perturbative induced energy loss, but pushing it to the extreme. Namely, they make two strong ad hoc assumptions which have no justification. First, it is assumed that pre-hadrons are produced always outside the nucleus. Second, the effect of induced energy loss is accounted for via a simple shift of the variable in the fragmentation function,

what is equivalent to the assumption that hadronization starts only after the leading parton leaves the nucleus.

Since the induced energy loss scenario is a popular explanation for the nuclear suppression of high-p_T events observed at RHIC, we confront some of the predictions of this model with data from HERMES. We sort out those observables which are sensitive to the model assumptions.

1.1 Why nuclear target?

Particles produced in hadronic collisions and detected at macroscopic distances carry limited information about the hadronization dynamics. The most important details are hidden at the early stage. Nuclear targets provide a unique opportunity to look at the early stage of hadronization at distances of few Fermi from the origin. A quark-gluon system originated from DIS propagates through the nuclear medium and interact with other nucleons. Modification of the differential cross section of particle production can bring forth precious information about the structure of the excited system and its space-time development.

We assume in what follows that Bjorken x is sufficiently large, $x \sim 0.1$, therefore the lepton interacts incoherently with only one bound nucleon, no shadowing is possible. Besides, this region is dominated by valence quarks, i.e. one can treat the DIS as electron-quark scattering with energy transfer, ν, to the knocked out quark. At small x dominated by the sea the process of DIS looks differently (in the nuclear rest frame), the virtual photon produces two jets, q and $\bar{q}$, which share the full energy ν. Therefore, the variable z_h, which is the fraction of ν transferred to the detected hadron, cannot reach the kinematic limit $z_h = 1$ for neither of the two jets, unless one of them takes the whole energy of the photon. This fact makes the nuclear ratio to fall at $z_h \to 1$ steeper than at large x. Besides, negative kaons which at large x are produced mainly from gluons, at small x are generated by the same mechanism as positive kaons. This, one should be cautious about the range of x involved into the analysis, and make a proper x-binning of DIS data.

One can also use the process of hadronization as a tool for probing the medium properties. This is the driving idea of so called "jet quenching" probe for creation of dense matter in relativistic heavy ion collisions [13]. This tool, however, can work properly only if the hadronization dynamics is reliably understood, which seems to be still a challenge.

1.2 Vacuum and induced energy losses

Energy loss is a hot topic nowadays, however, related discussions are confusing sometimes, since vacuum and induced energy losses are mixed up. Due to confinement an energetic parton cannot propagate in vacuum as a free particle, but hadronizes and produces a jet of hadrons. The parton shares its energy with the produced hadrons, therefore it is gradually losing energy. We call this *vacuum energy loss*. In the string model [14] the rate of energy loss should be constant, of the order of the string tension $\kappa = 1\,\mathrm{GeV/fm}$. Therefore, the energy loss rises linearly with time or length of the path,

$$- \Delta E_{vac}(L) = \kappa L \ . \tag{1}$$

If the parton originates from a hard reaction (DIS, high-p_T process, etc), gluon bremsstrahlung should be an additional source of energy loss. Indeed, as a result of a strong kick the parton should shake off a part of its color field with transverse frequencies controlled by the strength of the kick. Apparently, in this case energy loss may be very extensive and may substantially exceed the static value given by the string model. Amazingly, the radiative energy loss turns out to rise linearly with the path length [15] like in the string model,

$$- \Delta E_{vac}(L) = \frac{2}{3\pi}\,\alpha_s(Q^2)\,Q^2\,L \ . \tag{2}$$

This happens because the gluons lose coherence with the source, i.e. are radiated, at different time intervals.

In the case of hadronization inside a medium, an additional source of energy loss is interaction of partons with the medium. Due to multiple collisions the parton increases its transverse momentum squared linearly with the path length, since it performs Braunian motion in the transverse momentum plane. Experimentally, the broadening of transverse momentum is a rather small effect. For instance, the broadening measured in Drell-Yan reaction on a nucleus as heavy as tungsten is only $\Delta p_T^2 \approx 0.1\,\mathrm{GeV}^2$. Apparently, the induced energy loss [17] generated by such a small momentum transfer, is a small addition to the vacuum energy loss originated from a hard process (at least in a cold nuclear matter),

$$- \Delta E_{ind}(L) = \frac{3}{8}\alpha_s\,\Delta p_T^2\,L = \frac{3}{4}\,\alpha_s\,C(E)\,\rho_A\,L^2 \ , \tag{3}$$

where $C(E) = d\sigma_{\bar{q}q}(r_T, E)/dr_T^2\big|_{r_T=0}$ [18,19] is the derivative of the universal phenomenological dipole cross section; ρ_A is the nuclear density.

The intuitive interpretation of these results is rather straightforward. It takes time, called coherent time, to radiate a photon or gluon which have to get incoherent with the source [1],

$$t_c = \frac{2E\alpha(1 - \alpha)}{k_T^2} \ , \tag{4}$$

where k_T and α are the transverse momentum and fraction of energy taken away by the radiated quantum. According to Landau-Pomeranchuk principle radiation at long coherence times does not resolve the details of interaction, whether it was a single kick, or a few of them. What matters is the final transverse momentum of the parton. Since the additional transverse momentum gained by the parton due to multiple interactions in the nuclear medium is very small, the corresponding correction (induced) to the energy loss is small as well.

This is why it is not easy to see in data the effects of induced energy loss. In particular, the analysis of nuclear

effects in Drell-Yan reaction performed in [20] provided information about vacuum energy loss. Indeed, according to the kinematics of the E772/E866 experiments (and other experiments at lower energies) most of events correspond to a short coherence time for the Drell-Yan process which occurs nearly momentarily deep inside the nucleus. Prior to that the incoming hadron interacts softly on the face surface of the nucleus. This collision breaks down coherence of the projectile partons which start losing energy on the path from the soft collision point till the point where the Drell-Yan reaction takes place. One should expect the vacuum value for the rate of energy loss which is at least $-dE/dz \approx 1 \, \mathrm{GeV/fm}$ or higher, much larger than what one could expect for induced gluon bremsstrahlung. Indeed, the analyses [20] led to $-dE/dz = (2.8 \pm 0.4 \pm 0.5) \, \mathrm{GeV/fm}$, which is a summed effect of vacuum and induced energy losses.

Naively, one might expect that the effects of vacuum energy loss cancel out in the nucleus to nucleon ratio, since they are identical in the numerator and denominator. This is not correct, the vacuum energy loss controls the time scale of hadron production which has a great impact on nuclear effects (see next section).

1.3 Production and formation times

One should discriminate between formation of the final hadron and production of a colorless state which is not yet an eigen state of the mass matrix and may be projected to various hadronic wave functions. We call such states pre-hadrons and the related time scale *production time*, t_p. The properties of such pre-hadron states and their attenuation in nuclei have been intensively studied over last two decades, both theoretically and experimentally. It has been proven that such pre-hadrons of a reduced size are indeed produced, and that nuclei are indeed more transparent for such states. A clear signal of color transparency in DIS was observed recently in the HERMES experiment [21,22].

To form the hadronic wave function the constituents of the pre-hadron have to circle at least once along their orbits. Dilated by Lorentz transformation this time scale which we call *formation time*, t_f, is proportional to z_h, which is the fraction of the photon energy carried by the hadron. On the other hand, the production time t_p was proven in [23,4] and confirmed within the LUND model in [24] to vanish proportionally to $1-z_h$ at $z_h \to 1$. The latter property follows from energy conservation: the longer the hadronization process is lasting, the more energy is lost by the leading quark, unless its energy falls below the desired hadron energy. In particular, at $z_h = 1$ no energy loss for hadronization is allowed, so the colorless ejectile has to be created instantaneously.

1.4 What are the observables?

Nuclear medium affects the momentum distribution of the produced particles, which is called sometimes a modified fragmentation function $D_{eff}^A(z_h, p_T, Q^2, \nu)$, where p_T is the transverse momentum of the hadron, and ν and Q^2 are the energy and virtuality of the photon respectively. The energy dependence signals that QCD factorization is broken and D_{eff}^A cannot be treated as a fragmentation function, e.g. the evolution equations cannot be applied. Only at very large ν and Q^2 nuclear effects disappear and factorization is restored. In this trivial limit, however, all physical information we are interested in is missed.

Experimental results are usually presented in a simple form, as a ratio of the nucleus-to-nucleon hadron multiplicities,

$$R_A(z_h, p_T, Q^2, \nu) = \frac{dn(\gamma^*A \to hX)/dz_h d^2 p_T}{A \, dn(\gamma^*N \to hX)/dz_h d^2 p_T} \, . \quad (5)$$

Because of limited statistics this four-dimensional ratio is usually presented as one-dimensional ratios integrated over other variables. Some of correlations are, however, very informative. For instance, p_T dependence of the ratio binned in z_h brings forth precious information about the space-time pattern of hadronization (see Sect. 9.3).

Nuclear modification of the hadronic spectra was considered for high-p_T hadron production in [4,25], for DIS in [3,5,7] and for hadroproduction of leading particles on nuclei in [24,26].

1.5 What can we learn?

The questions, which can be answered in such an analysis are:

– *How long does it take to produce a pre-hadron?*
Nuclear suppression of hadron production, especially its z_h and p_T dependences, are sensitive to the production time t_p.

– *How does the produced pre-hadron evolve and attenuate in nuclear matter?*
Since we are interested in production of leading particles, we should forbid inelastic interaction of the produced colorless wave packet at times $t > t_p$. It would lead to a new hadronization process which ends up with a smaller value of z_h. The corresponding correction is easy to estimate and it turns out to be small. The condition of no interaction results in an attenuation of the produced wave packet in nuclear matter, but the absorption cross section of the pre-hadron may be different from the hadronic one. Particularly, in DIS with high photon virtuality Q^2 the produced wave packet may have a smaller transverse size, similar to what is known for exclusive particle production. Correspondingly, the color transparency effects [27, 28] should be important and we take care of that in what follows.

– *Does a fast quark attenuate in nuclear matter?*
At first glance an energetic quark should not attenuate since it cannot be stopped or absorbed in the medium. Multiple soft interactions can only rotate the quark in color space, while the energy loss is a small fraction of the quark energy. However, saying "attenuation" of a quark,

we mean the suppression of the production rate of the final hadron produced with a certain momentum, related to the quark interactions in the nuclear medium. In the string model any color-exchange interaction leads to formation of a new string, but with reduced initial energy. This fact results in a reduction of hadron production at large $z_h \to 1$ [6]. Moreover, the leading quark may pick up new strings due to presence of higher Fock components, giving rise to induced energy loss in this model [20]. If one tries to treat the reduced production rate of hadrons as an effective attenuation of the quark in the medium, the effective quark absorption cross section cannot be treated as an universal parameter. Its value essentially varies with geometry and kinematics [6]. In the present paper we include induced energy loss explicitly.

2 Lessons of the string model

Apparently, the nonperturbative string model cannot be a realistic approach to such a hard process as DIS. The model does not have any access to Q^2-dependence, color transparency, etc., the phenomena crucial for understanding the properties of in-medium hadronization. At the same time, the model is simple, very intuitive, and helps to understand the general features of the space-time development of hadronization.

As it was already mentioned, we assumed that data are taken at large Bjorken $x > 0.1$ to make sure that valence quarks in the target nucleon give the main contribution. A color string[1] formed between the quark and the debris of the target nucleon, is slowing down the former and speeding up the latter. Naively, one may think about a long string stretched across the nucleus. Instead, a very short object is propagating through the nucleus. Indeed, a simple kinematics shows that the maximal possible length of the string in the rest frame of the nucleus is,

$$L_{max} = \frac{m}{\kappa} , \qquad (6)$$

where m is the mass of the debris of the target nucleon (e.g. a diquark) attached to the slow end of the string. The string tension $\kappa = 1/(2\pi\alpha'_R) \approx 1\,\text{GeV/fm}$ is related to the slope α'_R of the Regge trajectories [14]. Since the nucleon debris are probably lighter than the nucleon, $L_{max} < 1$ fm. In reality the string should be even much shorter due to the Schwinger phenomenon, spontaneous $q\bar{q}$ pair production from vacuum breaking the string to shorter pieces.

Thus, a heavy but short string with the effective mass $M \approx \sqrt{s} = \sqrt{m_N^2 - Q^2 + 2m_N\nu}$ propagates through the nucleus. Due to $q\bar{q}$ pair production in the color field of the string light pieces of the string are chipped off, while the leading heavy part of the string keeps propagating on. Apparently, the leading quark is slowing down losing energy with a constant rate,

$$\frac{dE}{dt} = -\kappa , \qquad (7)$$

[1] Of course a one-dimensional string is an idealization. We neglect the transverse size of the color-flux tube [14], unless otherwise specified.

where $E(t)$ is the quark energy and $t = z$ are the time and longitudinal coordinate. Note that the rate of energy loss (7) is a constant which is independent of the quark flavor, energy and virtuality, and is invariant relative to longitudinal Lorentz boosts. Correspondingly, the total energy loss rises linearly with the length Δz of the path, $\Delta E = \kappa \Delta z$. The lost energy goes to acceleration of the target debris and production of new hadrons. The process of hadronization completes when the mass of the leading piece of the string is reduced by many decays down to the hadronic mass scale and the leading pre-hadron (or a cluster) is produced.

How does the production time depend on the initial quark energy ν and its fraction z_h carried by the produced hadron? For low energy hadrons it is short, but rises with their energy, $t_p \approx \nu z_h / 2\kappa$. One might think that such a linear z_h-dependence is an unquestionable truth since it is dictated by Lorentz time dilation. It was claimed, however, in [23,4] and confirmed within Lund model [24], that there is an opposite trend for leading hadrons, namely, the production time vanishes like $t_p = (1 - z_h)\nu/\kappa$ at $z_h \to 1$. Although it was first derived in the string model [23,4], this is a general property, since is dictated by conservation of energy. Indeed, unless color neutralization happens, i.e. a colorless system with energy $z_h\nu$ is produced, the leading quark keeps losing energy. Therefore, the smaller $(1 - z_h)$ is, the faster this process must be completed, otherwise the energy needed for the leading hadron production will be wasted.

Note, that the produced colorless object should be treated as a pre-meson. It may take a long time proportional to $z_h\nu$ to form the final hadron wave function. We call this formation time, and it is always longer than the production time, $t_f > t_p$.

Thus, we arrive at two different types of end-point behavior of the production time [23,4,24],

$$t_p = \begin{cases} \frac{\nu}{2\kappa} z_h & z_h \ll 1 \\ \frac{\nu}{\kappa} (1 - z_h) & 1 - z_h \ll 1 \end{cases} \qquad (8)$$

The concept of production time is crucial in the case of nuclear target: a colorless pre-hadron produced inside the nucleus should not interact (inelastically) on the way out of the nucleus, otherwise hadronization will be triggered, and the final hadron will emerge with a substantially reduced energy. Apparently, this condition leads to an attenuation which depends on the interaction cross section of the pre-hadron (see below). For this reason different processes on nuclei are suppressed near the kinematic limit $z_h \to 1$, for example, back-to-back high-p_T dihadron production, DIS, forward particle production in hadron-nucleus interactions, etc.

As was mentioned above, the production time (8) corresponds to creation of a fast colorless piece of the string, a pre-hadron, rather than the final hadron. The latter is supposed to have a wave function describing the specific distribution of quark momenta inside the hadron, different from the quark momentum ordering in the string. The wave function of the hadron is developing over a longer period of time (formation time), which is proportional to

the hadron energy, $z_h\nu$, rather than to $(1-z_h)\nu$. These two time scales are mixed up sometimes. However, nuclear attenuation is controlled mainly by the the production time (8), rather than by the formation time which has a moderate influence on nuclear effects. Nevertheless, we will include both effects in our calculations.

Another question which may be answered within the string model is how multiple interactions of the hadronizing quark at earlier stage, $t < t_p$ affects the hadron production rate? Sometimes [5,2] this attenuation is treated as absorption with an effective quark-nucleon cross section treated as a universal fitted parameter. However, the physical origin of such an attenuation discussed in [6] shows that it cannot be described in terms of a universal parameter like a quark absorption cross section. Indeed, every interaction of the leading quark leads to a new hadronization process starting from the very beginning, but with a reduced initial energy $E_q(z) = \nu - \kappa z$, where z is the distance covered by the quark. Since the energy of the final hadron is fixed, the variable of the fragmentation function should be redefined as, $z_h \Rightarrow z_h/(1-\kappa z/\nu)$. Apparently, the increase of z_h should lead to a suppression which depends on ν and z_h and cannot be treated as a universal parameter [6].

Besides, multiple quark interactions at $t < t_p$ induce an additional energy loss with a rate rising linearly with the path length z [20],

$$\frac{dE}{dz} = -\kappa\Big[1 + \langle n(z)\rangle\Big] , \qquad (9)$$

where $\langle n(z)\rangle = \sigma_{in}^{qN}\,\rho_A\,z$ is the mean number of collisions experienced by the quark over the distance z; σ_{in}^{qN} is the model dependent effective quark-nucleon inelastic cross section. The first term in (9), same as in (7), is the usual retarding force produced by the string, while the second term is due to additional strings created by multiple interaction of the quark. These extra terms correspond to higher Fock component of the quark and can be motivated within the dual parton model [29] (more details can be found in [20]).

Thus, the total energy loss on a distance L contains a correction $\propto L^2$.

$$\Delta E(L) = \kappa\,L\Big[1 + \frac{1}{2}\sigma_{in}^{qN}\rho_A\,L\Big] . \qquad (10)$$

In the additive quark model $\sigma_{in}^{qN} \sim 10\,\mathrm{mb}$, which is the same value as follows from the dual parton model [29]. Note, that this value is twice as large as in the more realistic model [30], which demonstrates that the dominant part of the hadronic cross section does not obey quark additivity.

It is questionable whether one can apply this phenomenology to DIS. At this point we feel that our unjustified assumption that soft interaction phenomenology, like the string model, is relevant for final state interaction in DIS has been pushed to the extreme, and we should consider a more realistic approach based on perturbative QCD.

3 Radiative energy loss: Hadronization in vacuum

3.1 Vacuum energy loss

When a high-momentum parton is produced in a hard reaction, it triggers gluon bremsstrahlung, which lasts until the moment of color neutralization. Gluons are not radiated instantaneously, but it takes time to lose coherence with the parent parton. This quantum-mechanical uncertainty called coherence time can be introduced differently. A strict definition comes within precise calculations and is related to interference between quanta radiated at different positions. For instance, two amplitudes of gluon radiation by a quark at different coordinates separated by the longitudinal distance Δz get phase shift $\Delta z q_L$, where $q_L = (M_{Gq}^2 - m_q^2)/2E_q$ is a difference between the longitudinal momenta of the quark and the produced quark-gluon final state which has effective mass squared,

$$M_{Gq}^2 = \frac{k_T^2 + \alpha m_q^2}{\alpha(1-\alpha)} . \qquad (11)$$

Here $\mathbf{k}_T$ and α are the transverse momentum and fraction of the light-cone momentum of the quark carried by the gluon; $E_q = \nu$ is the initial quark energy (we assume that Bjorken x is large and the quark gets the whole energy transfer).

Apparently, only those gluons can interfere, which are radiated within the coherence time interval, or coherence length (we assume $z = t$ and neglect the quark mass hereafter),

$$t_c \sim \frac{2\nu}{k_T^2}\alpha(1-\alpha) . \qquad (12)$$

This time may be also interpreted as the lifetime of the quark-gluon fluctuation, or as the formation time of radiation. At any rate, only those gluons may be treated as radiated during time t, which have coherence time $t_c < t$, otherwise they are still coherent with the quark and should be considered as a part of its color field.

Correspondingly, one can estimate the energy deposited into the radiation as

$$\Delta E(t) = \nu \int_{\lambda^2}^{Q^2} dk_T^2 \int_0^1 d\alpha\,\alpha\,\frac{dn_G}{dk_T^2 d\alpha}\,\Theta(t - t_c) \qquad (13)$$

where λ is an infrared cutoff. The number of radiated gluons $dn_G/d\alpha dk_T^2 = \gamma/\alpha k_T^2$, where $\gamma = 4\alpha_s(k_T^2)/3\pi$ [31,15]. As usual, we employ the approximation of soft radiation, $\alpha \ll 1$.

Equation (13) leads to a linear time dependence of energy loss,

$$\Delta E(t) = \frac{\gamma}{2}\,(Q^2 - \lambda^2)\,t \qquad (14)$$

i.e. the rate of energy loss is constant, like it is known for strings. This interesting observation was done in [15].
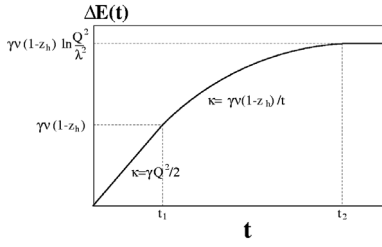
Fig. 1. Time-dependence of energy loss corresponding to (15). The notations are explained in the text

The radiated energy is distributed among produced hadrons, but we are interested in the most energetic one, leading hadron, which carries the largest fraction z_h of the initial momentum of the quark. This condition and energy conservation impose additional restrictions on the integration in (13), resulting in a different time-development of the hadronization and the energy loss.

If the leading hadron is produced with large z_h and includes the leading quark, none of the radiated gluon may leave with a fraction of the initial quark momentum exceeding $\alpha > 1 - z_h$. For instance, in the limiting case $z_h \to 1$ any radiation is forbidden, what leads to a so called Sudakov's suppression of the cross section. With decreasing z_h, this restriction gradually softens, but still should not be forgotten.

In order to estimate the time-dependence of radiative energy loss specified for the case of the leading hadron production we introduce energy conservation in (13) via step-function $\Theta(1 - z_h - \alpha)$. The result of integration reads,

$$
\Delta E(t) = \frac{\gamma}{2} t \, (Q^2 - \lambda^2) \, \Theta(t_1 - t)
$$
$$
+ \left\{ \nu \gamma (1 - z_h) \left[1 + \ln \left(\frac{t}{t_1} \right) \right] - \frac{\gamma}{2} \lambda^2 t \right\} \Theta(t - t_1) \Theta(t_2 - t)
$$
$$
+ \nu \gamma (1 - z_h) \ln \left(\frac{Q^2}{\lambda^2} \right) \Theta(t - t_2) \tag{15}
$$

where

$$
t_1 = \frac{2\nu}{Q^2}(1 - z_h) = \frac{1 - z_h}{x \, m_N} \,, \tag{16}
$$

$$
t_2 = \frac{Q^2}{\lambda^2} t_1 \,, \tag{17}
$$

and $x = Q^2 / 2 m_N \nu$ is Bjorken variable.

The time dependence of radiative energy loss is illustrated in Fig. 1 assuming $Q^2 \gg \lambda^2$. During the time interval $t < t_1$, the rate of energy loss is constant, $-dE/dt = \gamma Q^2/2$, exactly as in the case of (13), (14) with no restriction on the radiated energy.

Over a longer time interval, more energetic gluons can be emitted in accordance with (12) and the restriction $\alpha < 1 - z_h$ becomes effective. As a result, the loss of energy slows down to a logarithmic t-dependence. This implies that the rate of energy loss decreases as function of time as $dE/dt = -\gamma \nu (1 - z_h)/t$.

According to (15) at much longer times either very energetic gluons can be emitted (what may be forbidden by the condition $\alpha < 1 - z_h$), or gluons with very small

k_T. The latter are cut off in (13). This completely eliminates any energy loss at long times $t > t_2$ as one can see from (15) (see also Fig. 1). This sounds puzzling, but this is suppressed by a Sudakov-type factor. This suppression becomes active $t > t_1$, when the production of leading hadron with large z_h restricts the spectrum of radiation.

3.2 Leading hadron production

Summing up all the nonradiated gluons we get the following Sudakov's suppression

$$
S(t, z_h, Q^2, \nu) = \exp \left[-\tilde{n}_G(t, z_h, Q^2, \nu) \right] \,, \tag{18}
$$

where

$$
\tilde{n}_G(t, z_h, Q^2, \nu) = \gamma \int_{1 - z_h}^{1} \frac{d\alpha}{\alpha} \int_{\lambda^2}^{Q^2} \frac{dk_T^2}{k_T^2} [1 - \exp(-t/t_c)] \tag{19}
$$

is the number of gluons which have sufficiently short coherence time to be radiated during time interval t, but are conflicting with a leading hadron production since are too energetic, $\alpha > 1 - z_h$.

To be more realistic we should smooth out the step-function in (15). We assume that the radiation rate of gluons with coherence time t_c has a decay rate distribution,

$$
\frac{dP(t)}{dt} = \frac{1}{t_c} e^{-t/t_c} \,. \tag{20}
$$

Then the probability to radiate a gluon during time interval t is,

$$
P(t) = 1 - e^{-t/t_c} \,, \tag{21}
$$

which is a replacement for the step-function $\Theta(t - t_c)$ in (15) and (19).

The Sudakov formfactor, (18), substantially reduces the mean time interval of hadronization and the production time of the leading pre-hadron.

The estimate (1) for energy loss was obtained within the string model, which has no access to Q^2 dependence and assumes that the final hadron is immediately produced once the quark energy degraded down to $z_h \nu$. The perturbative QCD gives opportunity to develop a more detailed and profound model for hadronization and color neutralization. In the large N_c limit each radiated gluon is equivalent to a $q\bar{q}$ pair, and the products of gluon bremsstrahlung can be seen as a system of colorless dipoles (compare with [32,33]). It is natural to assume that the leading hadron originates from the color dipole, which includes the leading quark and the antiquark from the last radiated gluon. In the $1/N_c$ approximation they are automatically tuned in color, i.e. this pair is colorless. This $q\bar{q}$ dipole is to be projected on the hadron wave function, $\Psi_h(\beta, l_T)$, where β is the fractions of the hadron light-cone momentum carried by one of the quarks, and l_T is the transverse momentum of the quarks in the hadron.

Let us evaluate the distribution function $W(t, z_h, Q^2, \nu)$ for production time t of a pre-meson,

$$W(z_h, t, Q^2, \nu) = N \int\limits_0^1 \frac{d\alpha}{\alpha} \, \delta \left[z_h - \left(1 - \frac{\alpha}{2}\right) \frac{E_q(t)}{\nu} \right]$$

$$\times \int\limits_{\Lambda^2}^{Q^2} \frac{dk_T^2}{k_T^2} \, \frac{\exp(-t/t_c)}{t_c} \int dl_t^2 \, \delta \left[l_T^2 - \frac{9}{16} k_T^2 \right]$$

$$\times \int\limits_0^1 d\beta \, \delta \left[\beta - \frac{\alpha}{2 - \alpha} \right] |\Psi_h(\beta, l_T)|^2 \, S(z_h, t, Q^2, \nu) . \quad (22)$$

Here α is the fraction of the quark light-cone momentum carried by the gluon emitted at the time t by the quark of energy $E_q(t) = \nu - \Delta E(t)$. The mean radiation time of this gluon t_c is given by (12). Assuming that the radiated gluon splits to a $\bar{q}q$ pair which shares the gluon momentum in equal parts, we conclude that the leading colorless $q\bar{q}$ pair is produced with an energy $E_q(t)(1-\alpha/2)$. On the other hand, this must be the observed energy $z_h\nu$ of the produced hadron, the condition controlled by the first δ-functions in (22). The transverse momentum l_T of the quark and the antiquark within the colorless dipole is related to k_T as $\mathbf{l}_T = 3\mathbf{k}_T/4$, while the fraction of the hadron light-cone momentum carried by the quark is $\beta(t) = \alpha(t)/[2 - \alpha(t)]$. This is why we need the last two δ-functions in (22). Normalization factor N in (22) cancels in ratio (5), so we do not specify it.

Note that (22) has a probabilistic structure, instead of projecting the production amplitude on the hadron wave function, we convolute the squares of them. This simplification is related to to our need to include the time development of hadronization and make use of the coherence time. To do it correctly one should work with amplitudes taking care of interferences at all stages. In principle, this can be done within the path integral approach (partially applied below), however, technically it is so complicated that exact solution of this problem does not look feasible at present. Nevertheless, we will see in what follows that the approximation (22) does a good job describing data.

We use the parameterization for the hadronic wave function in (22) in the form of the asymptotic light-cone meson wave function,

$$\Psi_h(\beta, l_T^2) \propto \frac{\beta(1 - \beta)}{\beta(1 - \beta) + a_0} \exp \left[-\frac{R_h^2 \, l_T^2/8}{\beta(1 - \beta) + a_0} \right], \quad (23)$$

where $R_h^2 = 8\langle r_h^2 \rangle_{em}/3$ is related to the mean hadronic electromagnetic radius squared, $\langle r_h^2 \rangle_{em}$. Normalization is not important since it can be absorbed into the factor N in (22). The parameter a_0 in (23) incorporates confinement for highly asymmetric $q\bar{q}$ configurations with $\beta \to 0, 1$. We fix this parameter demanding the mean charge radius of the hadron to be correctly reproduced,

$$\langle \rho^2 \rangle = \frac{\int \frac{d\beta}{\beta (1-\beta)} \int d\rho^2 |\Psi_h(\beta, \rho)|^2 \, \rho^2}{\int \frac{d\beta}{\beta (1-\beta)} \int d\rho^2 |\Psi_h(\beta, \rho)|^2} = \frac{8}{3} \langle r^2 \rangle_{em} , \quad (24)$$
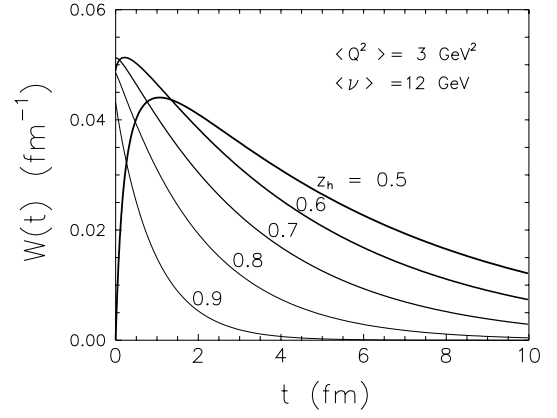

Fig. 2. Distribution of the hadron production time at $\nu = 12\,\text{GeV}$, $Q^2 = 3\,\text{GeV}^2$ and $z_h =$ 0.5-0.9

where $\Psi_h(\beta, \rho)$ is the hadronic wave function in coordinate representation, i.e. the Fourier transformation of (23). For production of pions with $\langle r^2 \rangle_{em} = 0.44 fm^2$ [34] we found $a_0 = 1/12$.

Examples for the production-time distribution $W(t)$ at $< \nu >= 12\,\text{GeV}$, $< Q^2 >= 3\,\text{GeV}^2$ and different z_h are presented in Fig. 2 [2]. We see that as function of z_h the mean production time decreases similar to the expectations of the string model (5) (but with different value of κ), what is not a surprise, since this behavior reflects conservation of energy.

There are no data, of course, for $W(t, z_h)$ to compare with, but the integral over t at fixed z_h is the probability to produce the hadron with energy $z_h\nu$. This probability is the fragmentation function which is rather well known phenomenologically.

$$\tilde{D}_{h/q}(z_h, Q^2) = \int\limits_0^\infty dt \, W(t, z_h, Q^2) . \quad (25)$$

Tilde here means that this function describes fragmentation of a quark only to a (leading) hadron which includes the parent quark.

Now we can fix the normalization factor N in (22). In fact, the normalization of $\tilde{D}_{h/q}$ is different from that for the conventional fragmentation function which is normalized to the particle multiplicity, $\int_0^1 dz_h D_{h/q}(z_h, Q^2) = \langle n_h \rangle$. Apparently, only one hadron in the produced jet contains the original quark, therefore,

$$\int\limits_0^1 dz_h \, \tilde{D}_{h/q}(z_h, Q^2) = 1. \quad (26)$$

Now we are in a position to compare the modeled fragmentation function with a realistic phenomenological one. In view of the specifics of our model which is designed to reproduce production of leading hadrons, we may expect

---

[2] Note that a function, $t W(t)$ was plotted in Fig. 1 of [1], but factor t was missed in the notations.
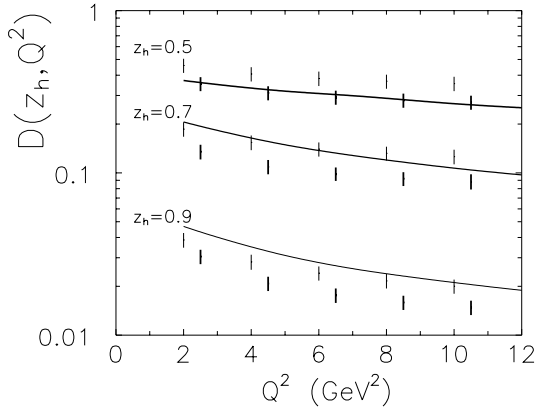
Fig. 3. The model prediction for the fragmentation function $\tilde{D}(z_h, Q^2)$ in comparison with parametrizations fitted to data, [35] (*thin vertical bars*) and [36] (*thick bars*)

agreement only at large z_h, probably $z_h > 0.5$. Our calculations for Q^2 dependence of $\tilde{D}_{h/q}(z_h, Q^2)$ at different z_h are depicted in Fig. 3, and are compared with the popular parametrizations fitted to data, [35] and [36] shown by thin and thick bars respectively. The difference between the parametrizations may be treated as a systematic uncertainty. The model reproduces the phenomenological fragmentation function rather well. This encourages us to apply this approach to nuclear targets as well.

4 Evolution and attenuation of the pre-hadron in nuclear environment

Production of a leading colorless pre-hadron with the detected momentum completes the process of hadronization. The further propagation of the pre-hadron in vacuum and formation of the hadronic wave function have no observable effect, since leads only to a phase shift. This changes drastically in presence of an absorptive medium. In this case the production time t_p is of a special importance. Indeed, when color neutralization happens and a pre-hadron with the desired energy, $z_h \nu$, is produced, any subsequent inelastic interaction in the medium gives rise to a new hadronization process, and the quark energy substantially degrades down to a lower value of z_h. This means that the pre-hadron should have been produced with a larger $z_h' > z_h$, i.e. with a smaller probability. Such a suppression of the hadron production rate turns out to be so strong that we can neglect these double-step processes.

If the energy of the pre-hadron ($\bar{q}q$ dipole) is sufficiently high to freeze the transverse $\bar{q}q$ separation (due to Lorentz time dilation) for the time of propagation through the medium, then the survival probability of the pre-hadron, which we also call nuclear transparency, gets the simple eikonal form,

$$ Tr = \left| \frac{\langle \Psi_h(r_T) | \exp\left[-\frac{1}{2}\sigma_{\bar{q}q}^N(r_T) T_A\right] | \Psi_{\bar{q}q}(r_T) \rangle}{\langle \Psi_h(r_T) | \Psi_{\bar{q}q}(r_T) \rangle} \right|^2, \quad (27) $$
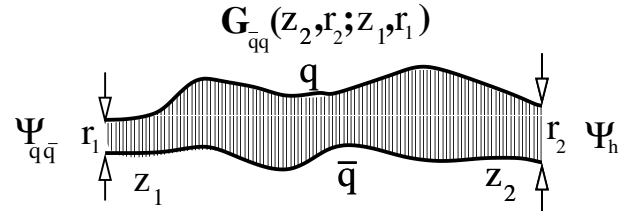

Fig. 4. The light-cone Green function $G_{\bar{q}q}(z_2, \mathbf{r}_2; z_1, \mathbf{r}_1)$ describing propagation of a $\bar{q}q$ pair over all possible paths in a medium between points with coordinates z_1 and z_2

where T_A is already introduced nuclear thickness, given in this case by integral of the medium density along the path of the dipole, $T_A(z_1, z_2) = \int_{z_1}^{z_2} dz \, \rho_A(z)$. The universal dipole-nucleon cross section, $\sigma_{\bar{q}q}^N(r_T)$, was introduced earlier. $\Psi_{\bar{q}q}(r_T)$ and $\Psi_h(r_T)$ are the light-cone wave functions of the initial $\bar{q}q$-dipole (pre-hadron) and the final hadron respectively.

In the case of medium energies (HERMES, Jefferson Lab) the dipole size may substantially fluctuate during propagation through the nucleus and nuclear transparency might substantially differ from (27). The rigorous quantum-mechanical approach incorporating all effects of fluctuations should include all possible trajectories of the quark and antiquark, rather than just fixed quasi-classical ones. This path integral technique leads to an expression for the survival probability of a dipole in a medium similar to (27). However, the exponential attenuation factor in the numerator must be replaced by the light-cone Green function, $G_{\bar{q}q}(z_2, \mathbf{r}_2; z_1, \mathbf{r}_1)$, which describes propagation of the $\bar{q}q$ pair with initial and final separations $\mathbf{r}_1$ and $\mathbf{r}_2$, between points with longitudinal coordinates z_1 and z_2 [37,38,22], as is illustrated in Fig. 4. Then the nuclear transparency (27) takes the form,

$$ Tr(z_1, z_2) = \left| \frac{\int d^2 r_1 d^2 r_2 \Psi_h^*(r_2) G_{\bar{q}q}(z_2, \mathbf{r}_2; z_1, \mathbf{r}_1) \Psi_{\bar{q}q}(r_1)}{\int d^2 r \, \Psi_h^*(r) \Psi_{\bar{q}q}(r)} \right|^2. $$
$$ (28) $$

The Green function satisfies the two-dimensional light-cone Schrödinger equation,

$$ i \frac{d}{dz_2} G_{\bar{q}q}(z_2, \mathbf{r}_2; z_1, \mathbf{r}_1) = \left[\frac{m_q^2 - \Delta_{r_2}}{2 E_h \beta (1 - \beta)} + V_{\bar{q}q}(z_2, \mathbf{r}_2, \beta) \right] $$
$$ \times G_{\bar{q}q}(z_2, \mathbf{r}_2; z_1, \mathbf{r}_1), \quad (29) $$

with the boundary condition $G_{\bar{q}q}(z_2, \mathbf{r}_2; z_1, \mathbf{r}_1)|_{z_2 = z_1} = \delta^{(2)}(\mathbf{r}_1 - \mathbf{r}_2)$. Here $E_h = z_h \nu$ is the hadron energy, and β is the fraction of the hadron light-cone momentum carried by the quark. The first, kinetic, term in squared brackets is responsible for the phase shifts which are related to quark masses, m_q, and their transverse motion described by Laplacian Δ_r acting on coordinate r.

The imaginary part of the light-cone potential in (29),

$$ \mathrm{Im}\, V_{\bar{q}q}(z, \mathbf{r}, \beta) = -\frac{1}{2} \sigma_{\bar{q}q}^N(r) \rho_A(z), \quad (30) $$

is responsible for attenuation of the $\bar{q}q$ in the medium, while the real part represents the interaction between the

q and $\bar{q}$. The latter is supposed to provide the correct light-cone wave function of the final meson. For the sake of simplicity we use the oscillator form of the potential,

$$\mathrm{Re}\, V_{\bar{q}q}(z,\mathbf{r},\beta) = \frac{a^4(\beta)\,\mathbf{r}^{\,2}}{2\,E_h\,\beta(1-\beta)}\ ,\qquad(31)$$

which leads to a Gaussian r-dependence of the light-cone wave function of the meson ground state. The shape of the function $a(\beta)$ was discussed in [39], and fixed by photoproduction data $a^2(\beta) = a_0^2 + a_1^2\beta(1-\beta)$, where $a_0^2 = v^{1.15} \times (112\,\mathrm{MeV})^2$; $a_1^2 = (1-v)^{1.15} \times (165\,\mathrm{MeV})^2$, and v takes any value in the interval $0 < v < 1$.

If we assume also that the small-r dependence for the dipole cross section, $\sigma_{\bar{q}q}^N(r) = C(E_h)\,r^2$, then (29) has an analytical solution [40],

$$G_{\bar{q}q}(z_2,\mathbf{r}_2;z_1,\mathbf{r}_1) = \frac{a^2(\beta)}{2\,\pi\,i\,\sin(\xi\,\Delta z)}$$

$$\times \exp\left\{\frac{i\,a^2(\beta)}{\sin(\xi\,\Delta z)}\left[(r_1^2 + r_2^2)\cos(\xi\,\Delta z) - 2\,\mathbf{r}_1\cdot\mathbf{r}_2\right]\right\}$$

$$\times \exp\left[-\frac{i\,m_q^2\,\Delta z}{2\,E_h\,\beta\,(1-\beta)}\right]\ ,\qquad(32)$$

where $\Delta z = z_2 - z_1$ and

$$\xi = \frac{\sqrt{a^4(\beta) - i\beta(1-\beta)E_h\,C(E_h)\,\rho_A}}{E_h\,\beta(1-\beta)}\ ,\qquad(33)$$

This solution is valid only for a medium with a constant density. However, using the recurrent relations between Green functions for different space intervals one can solve analytically the problem for a varying density as well [37].

5 Nuclear attenuation caused by absorption

We assume that the colorless $\bar{q}q$ pair (pre-hadron) produced at distance l_p from the DIS point has Gaussian distribution of transverse separations with the mean transverse size related to the inverse value of the mean transverse momentum of the quarks,

$$\langle r_1^2\rangle = \frac{4}{\langle l_T^2(t_p)\rangle} = \frac{64}{9\,\langle k_T^2(t_p)\rangle}\qquad(34)$$

where

$$\langle k_T^2(t)\rangle = \frac{\int_{\lambda^2}^{Q^2} dk_T^2\left[dW(t,z_h,k_T^2,\nu)/d\ln(k_T^2)\right]}{\int_{\lambda^2}^{Q^2} dk_T^2\left[dW(t,z_h,k_T^2,\nu)/dk_T^2\right]}\ .\qquad(35)$$

A $\bar{q}q$ dipole with starting value of transverse size $r_1(t_p)$ experiences evolution, forming the hadronic wave function and getting through the filtering process in the nuclear medium which absorbs more effectively dipoles of larger size. If it were in vacuum, it would take formation time t_f which can be estimated as

$$t_f \approx \frac{2z_h\nu}{m_{h'}^2 - m_h^2}\ ,\qquad(36)$$

where h' is the first radial excitation of the hadron h. As was mentioned in the introduction, the formation time linearly rises with z_h, while the production time vanishes at $z_h \to 1$.

The effective fragmentation function modified by the survival probability (transparency) of the pre-hadron in the nuclear matter reads,

$$D_{eff}^A(z_h,Q^2,\nu) = \int d^2\mathbf{b}\int_{-\infty}^{\infty} dz\,\rho_A(\mathbf{b},z)$$

$$\times \int_0^{\infty} dt\,W(t,z_h,Q^2,\nu)\,Tr(b,z+t,\infty)\ .\qquad(37)$$

In the case of vanishing absorption, $\sigma_{\bar{q}q}^N \to 0$, this fragmentation function is identical to one on a free nucleon, except is A times larger. Ratio of the effective fragmentation function on a nuclear target to one on a free nucleon is identical to the experimental definition (5).

As was mentioned, we use the dipole approximation, $\sigma_{\bar{q}q}^N(r) = C\,r^2$. Factor C is proportional to the inverse mean hadron radius squared related to the parameters of the oscillatory potential,

$$C = \frac{1}{2}\,m_q\,\omega\,\sigma_{tot}^{hN}\ ,\qquad(38)$$

where $\omega = (m_{h'} - m_h)/2$ is the oscillatory frequency. For production of leading pions we took $\omega = 0.3\,\mathrm{GeV}$ and $m_q = 0.2\,\mathrm{GeV}$ which is constrained by the mean charge pion radius,

$$\langle r_T^2\rangle_h = \frac{2}{m_q\,\omega} = \frac{8}{3} < r^2 >_{ch}\ ,\qquad(39)$$

and nuclear shadowing data [41]. Using $\sigma_{tot}^{\pi N} = 25\,\mathrm{mb}$ we arrive at $C \sim 1.9$.

6 Comparison with data

Unfortunately low statistics of HERMES data does not allow to perform a multi-dimensional comparison with the theory. One should integrate over all variables except one to get data with reasonable errors.

6.1 Energy dependence of nuclear effects

The results of numerical calculations for energy dependence of the ratio of nuclear-to-nucleon cross sections for leading pion production integrated over z_h, p_T and Q^2 are depicted by dashed curve in Fig. 5 in comparison with with HERMES data. We ignored the induced energy loss in these calculations and integrated over $z_h > 0.5$. Since the data are integrated over $z_h > 0.2$, this may cause some difference.

It is clear why nuclear suppression is maximal at low energies and has a tendency to vanish with increasing energy (data from EMC experiment [42] at much higher energies indeed demonstrate no nuclear effects). As we discussed in previous sections, hadronization process is completed by production of the leading colorless wave packet,
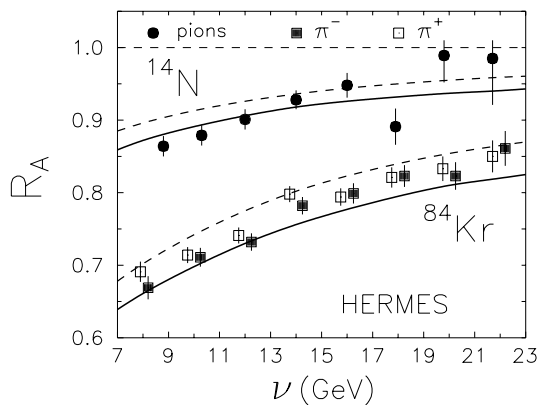
Fig. 5. Comparison of the model calculations for the ν- dependence of nuclear suppression $R_{N^{14}}$ (5) integrated over z_h with the HERMES data [2]. The solid and dashed curve are the model predictions for nuclear suppression with and without induced radiation to be taken into account, respectively

Fig. 6. Comparison of the model calculations for the z_h-dependence of nuclear suppression R_{Cu} (5) at the energy $<\nu>= 35\,\mathrm{GeV}$ (*dashed curve*) and $<\nu>= 145\,\mathrm{GeV}$ (*solid curve*) with the EMC data [42,44]. Calculations are done at $Q^2 = 11\,\mathrm{GeV}^2$

which is then evolving into the final hadron over the formation time t_f given by (36). If color neutralization happens outside the nucleus ($t_p > R_A$), the evolution leads only to a phase shift, resulting in no nuclear effects, as long as we neglect the induced energy loss.

On the other hand, the evolution may cause a strong attenuation if the wave packet is produced inside the nuclear target, as it happens at low energies where $t_p < R_A$. At higher energies t_p rises leaving less room for absorption. Besides, the formation time t_f rises too, and the initial small size, $r_T \sim 1/Q$, of the pre-hadron is evolving slower, leading to a lesser attenuation due to color transparency. Both effects lead to a stronger nuclear suppression at small than at high energies in accordance with data from HERMES [2] (Fig. 5), SLAC [43] and EMC [42, 44] experiments.

6.2 z_h-dependence of nuclear effects

Even at high energies the production time shrinks at large $z_h \to 1$ according to (8) and Fig. 2. Thus, at large z_h the path available for absorption of the pre-hadron reaches maximal length resulting in a strongest nuclear suppression. Such a shape of nuclear ratio falling toward $z_h = 1$ has been expected since 30 years ago [4,24], but high energy experiments could not reach sufficiently large values of z_h. Our predictions [1] are compared with EMC data in Fig. 6. We see that the interval of z_h where l_p is short absorption is at work, is rather short and squeezed towards $z_h = 1$. This is because the energy is too high, but absorption is at work only if $l_p \propto \nu(1 - z_h)$ is shorter than the nuclear size, what needs quite a small $(1 - z_h) \propto 1/\nu$.

This is why measurements at much lower energies of HERMES were proposed in citeknp in order to detect this effect. Fig. 7 demonstrates HERMES data for nitrogen and krypton in comparison with our predictions shown by dashed curves for the case of pure absorption. This is the first experimental confirmation for the longstanding prediction of vanishing production length at $z_h \to 1$.

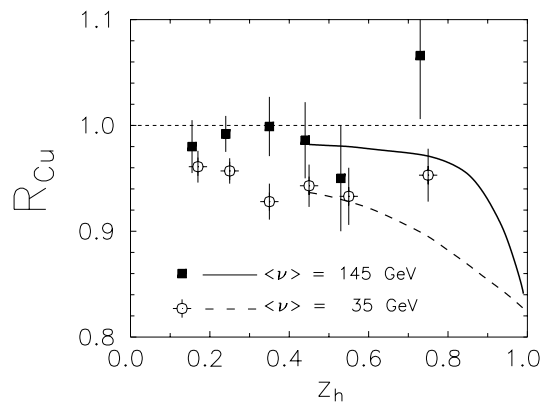Note, however, that even at $z_h \to 1$ nuclear suppression vanishes if both ν and Q^2 are sufficiently large. This is demanded in QCD by k_T-factorization and is correctly reproduced by our model. Indeed, at high Q^2 the initial size of the pre-hadron is very small, and it remains small long enough if the energy is high. Then color transparency eliminates nuclear effects.

6.3 Q^2 dependence of nuclear effects

At least two effects are sensitive to a variation of Q^2, color transparency and the production length. Apparently, the initial size of the pre-hadron shrinks at larger Q^2 and the nuclear matter becomes more transparent, i.e. the survival probability for the pre-hadron increases. At the same time, the production length l_p contracts because of rising vacuum energy loss, and provides a longer path available for absorption. This effect leads to a stronger nuclear suppres-
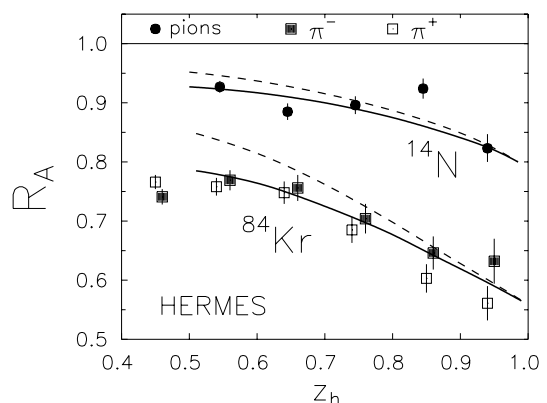

Fig. 7. Model predictions for the z_h- dependence of nuclear ratios R_{14N} (5) and R_{84Kr} calculated at values of $<\nu>$ and Q^2 corresponding to the measurements at HERMES. The *solid and dashed curve* are the model predictions with and without inclusion of induced radiation, respectively
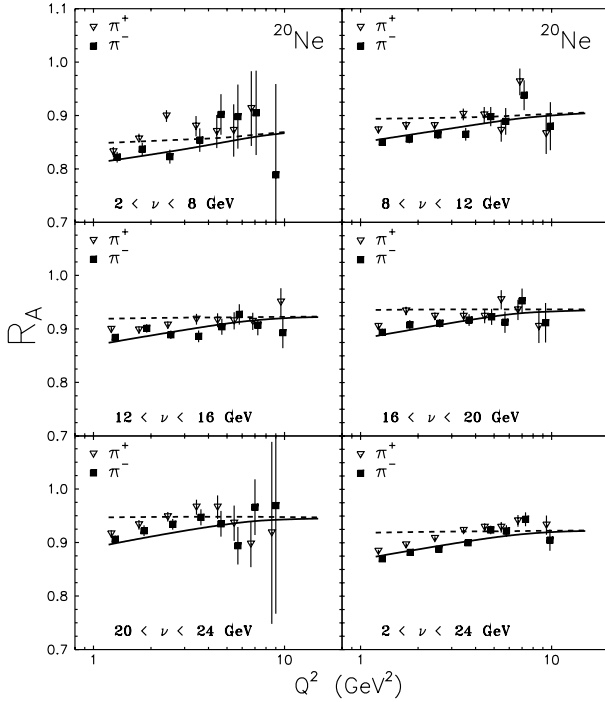
Fig. 8. Comparison of the model calculations for the Q^2- dependence of the ratio R_{Ne} of cross sections integrated over z_h with preliminary data from the HERMES experiment [45]. The *solid and dashed curve* are the model predictions with and without corrections for induced gluon radiation respectively

sion at larger Q^2. Thus, the two effects work in opposite directions and may partially or fully compensate each other. Indeed, it nearly happens: our predictions for pure effect of absorption depicted by dashed curves in Fig. 8 for neon demonstrate a rather weak Q^2-dependence. Although the Q^2-dependence demonstrated by the HERMES data is not steep either, one can see some difference. We will come to this point later after inclusion of corrections related to induced energy loss.

7 Corrections for induced gluon radiation

Multiple interactions of the quark during the time interval between the DIS point and production of the colorless pre-hadron cannot stop or absorb the quark, which keeps propagating through the medium rotating in the color space. Nevertheless, the additional soft kicks gained by the quark enforce it to shake off more gluons. This additional gluon radiation induced by the medium increases the loss of energy compared to vacuum. We calculate the induced energy loss in accordance with (3) where Δp_T^2 can be taken from data on p_T-broadening in Drell-Yan reaction, or from calculations (see next section) which agree with data. Then one should add this induced energy loss to the vacuum one, i.e. to replace $\Delta E_{vac}(t) \Rightarrow \Delta E_{vac}(t) + \Delta E_{ind}(t)$ for the time-dependent quark energy, $E_q(t) \equiv \nu - \Delta E(t)$ in (22).

Another modification of our calculations caused by p_T-broadening in the medium is the modification of the hard

scale. Namely, one should replace $Q^2 \Rightarrow Q^2 + \Delta p_T^2(t)$ in (18) for the Sudakov factor and in (22).

Both corrections enhance nuclear suppression, i.e. diminish the nuclear ratio. The results are shown by solid curves in Figs. 5, 7, 8 and 12. Apparently, these induced energy corrections vanish if $l_p \to 0$. This happens at $z_h \to 1$ and at maximal Q^2. Indeed, the dashed and solid curves in Figs. 7, 8 and 12 coincide in these limits.

8 Nuclear broadening of the transverse momentum distribution

According to the perturbative QCD treatment of induced energy loss, it is caused by the broadening of transverse momentum of the quark initiating a jet during the hadronization process (at $t < t_p$). At longer time intervals, $t > t_p$, the produced pre-hadron carries undisturbed information about the quark transverse momentum (since it has no interactions) which thus can be directly measured. Comparison with theoretical predictions seems to be of special importance.

A parton propagating through a medium experiences multiple interactions in the medium and performs Braunian motion in transverse momentum plane. As a result, the mean transverse momentum squared of the quark linearly rises with the path length. Quantitatively this process has been successfully described within the light-cone dipole approach [18,19] (otherwise, most of models just fit the data to be explained). If the DIS takes place on a nucleon with coordinates $(\mathbf{b}, z)$, the medium modified transverse momentum distribution is expressed in terms of the universal cross section of a $\bar{q}q$ dipole with a nucleon,

$$\frac{dN_q^A(b,z)}{d^2 p_T} = \int d^2 r \, d^2 r' \, \Omega_q(\mathbf{r}_T, \mathbf{r}_T') \exp\left[i\mathbf{p}_T(\mathbf{r}_T - \mathbf{r}_T')\right]$$

$$\times \exp\left[-\frac{T_A(b, z, z + l_p)}{2} \sigma_{\bar{q}q}^N(\mathbf{r}_T - \mathbf{r}_T', \nu)\right]. \quad (40)$$

Here $T_A(b, z, z + l_p) = \int_z^{z+l_p} dz' \, \rho_A(b, z')$ is the nuclear thickness function; $\sigma_{\bar{q}q}^N(r_T, \nu)$ is the phenomenological dipole cross section fitted to data for the proton structure function and photoabsorption cross section. It includes nonperturbative effects, as well as all corrections for gluon radiation (which give rise to the energy dependence of the cross section) also contributing to the broadening of the quark transverse momentum.

The quark density matrix in coordinate representation,

$$\Omega_q(\mathbf{r}_T, \mathbf{r}_T') = \frac{k_0^2}{\pi} \exp\left[-\frac{k_0^2}{2}(r_T^2 + r_T'^2)\right], \quad (41)$$

describes the initial distribution of the quark in the target nucleon. It controls the transverse momentum distribution of the valence quark emerging from DIS on a free nucleon. Therefore, the mean transverse momentum is of the order of the inverse proton size, i.e. is rather small, $k_0 \sim \Lambda_{QCD}$. Usually data on hard processes need a much larger primordial transverse momentum. This effect is related to

the next-to-leading order corrections related to hard gluon emission. Since we explicitly include gluon radiation in our model, additional next-to-leading order corrections would lead to double counting.

Note that our parameter-free approach successfully explained available data for the Cronin effect in pA collisions predicted it for $d - Au$ collisions at RHIC [22]. Data for nuclear broadening in Drell-Yan reaction also are well reproduced [19].

To get the hadron transverse momentum distribution we should convolute the quark p_T-distribution, (40) calculated without the exponential factor, with the fragmentation function $D_{h/q}(z_h, p_T)$,

$$
\frac{1}{\sigma_{DIS}^N} \frac{d\sigma_{DIS}^N(\gamma^* N \to hX)}{d^2 p_T} = \int d^2 k_T \, d^2 q_T \, \frac{dN_q^N}{d^2 q_T}
$$
$$
\times \frac{dD_{h/q}(z_h, k_T^2)}{d^2 k_T} \delta\left(\mathbf{p}_T - \mathbf{q}_T - \frac{\mathbf{k}_T}{2}\right) . \tag{42}
$$

Now we can make use of our model for the vacuum fragmentation function $\tilde{D}_{h/q}(z_h, Q^2)$, (26), and calculate the mean momentum squared of the produced meson. It hardly varies with Q^2 within the kinematic range corresponding to HERMES data. We found $\langle p_T^2 \rangle = \langle k_T^2 \rangle / 4 + k_0^2 = 0.3\,\text{GeV}^2$, where $k_0 = 0.2\,\text{GeV}$. This result agrees with the p_T-distribution of hadrons measured at SLAC [46] at energies overlapping with the HERMES energy range.

The p_T-dependence of the effective fragmentation function in nuclear medium, according to (37), reads,

$$
\frac{A}{\sigma_{DIS}^A} \frac{d\sigma_{DIS}^A(\gamma^* A \to hX)}{d^2 p_T} = \int d^2\mathbf{b} \int_{-\infty}^{\infty} dz \, \rho_A(\mathbf{b}, z)
$$
$$
\times \int_0^{\infty} dt \, Tr(b, z+t, \infty) \int d^2 k_T \, d^2 q_T \, \frac{dN_q^A(b, z)}{d^2 q_T}
$$
$$
\times \frac{dW(t, z_h, k_T^2, \nu)}{d^2 k_T} \delta\left(\mathbf{p}_T - \mathbf{q}_T - \frac{\mathbf{k}_T}{2}\right) \tag{43}
$$

We also included the small effect of Fermi motion in the nucleus.

The calculated ratio of the two distributions, nucleus-to-nucleon, is depicted in Fig. 9 for nitrogen and krypton in comparison with data from the HERMES experiment [2]. The model successfully reproduces the data with no adjustment.

9 Disentangling absorption and induced energy loss

The production length is a fundamental characteristics of the early stage of hadronization, and it is important to sort out those observables which are sensitive to l_p.

Such observables could also help to disentangle different models of hadronization. The current estimates of l_p within different models (strings [4,24,2,8], pQCD [1]) are pretty close and show that l_p is rather short compared to
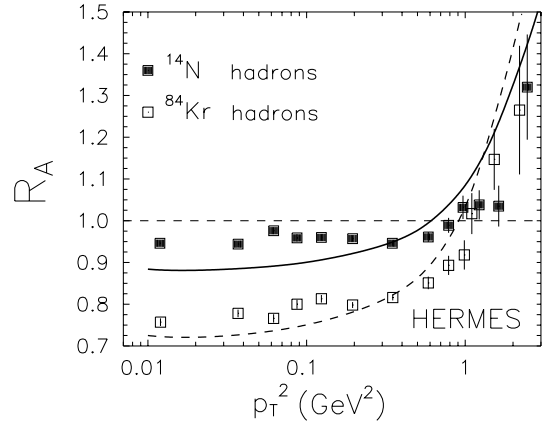

Fig. 9. The p_T-dependent nucleus-to-nucleon ratios of the cross sections of hadron production in DIS on nitrogen (*solid curve*) and krypton (*dashed curve*) in comparison with HERMES data

the nuclear sizes for the kinematics of the experiments at HERMES [2] and especially at Jefferson Lab [47]. At the same time, some models [11] make an assumption that color neutralization happens always outside the nucleus. Although this is an ad hoc assumption with no justification, would be useful to confront it with a direct experimental evidence.

9.1 Flavor dependence

The survival probability for the produced pre-hadron depends on the wave function of the final hadron, as one can see in (28). Also intuition tells us that the projection to a wave function with a larger mean radius should emphasizes larger $\bar{q}q$ separations in the pre-hadron, leading to a stronger absorption. Since pion has a larger radius than the kaon, the former is expected to be produced with a stronger nuclear suppression, than the latter. This may be a good signature for absorptive effects and shortness of l_p. On the contrary, in the case of $l_p \gg R_A$ there should be no sensitivity to the hadronic size.

HERMES experiment has provided recently high quality data for hadron production with particle identification [2]. Here we concentrate only on production of pions and positive kaons, since negative kaons and antiprotons do not contain valence quarks common with the target nucleon, while proton production is much contaminated with the target nucleons.

Our predictions for the production rates of positive kaons and pions integrated over z_h are depicted in Fig. 10 as function of photon energy together with recent data from HERMES. The two curves are different only by the value of the charge radius, $\langle r^2 \rangle_{ch}$ (kaon or pion) used in calculations.

Data confirm the expected identical suppression for positive and negative pions, and less attenuation for kaons. Although our calculations underestimate kaons, this is due to the difference in the bottom limit of integration over z_h, $(z_h)_{min} = 0.2$ in the data, and 0.5 in our calculations. At
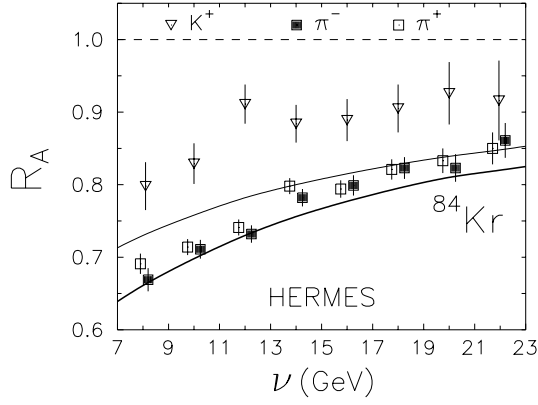
Fig. 10. Comparison of nuclear effects for kaon (*thin curve*) and pion (*thick curve*) productions as function of energy in comparison with HERMES data

small z_h kaons are copiously produced via reaction $\pi p \to K\Lambda$ which has a very low energy threshold. It would make sense if experimental data used a larger value of $(z_h)_{min}$.

Although the alternative model, the energy loss scenario, is not sensitive to the hadronic radius, one may expect a difference in quark fragmentation functions for $q \to \pi$ and $q \to K$, where q is a light quark, u or d. Indeed, the end-point behavior of fragmentation function, at $z_h \to 1$, is dictated by the Regge phenomenology,

$$D_{\pi/q}(z_h) \propto (1-z_h)^{1-\alpha_\rho(0)} = (1-z_h)^{0.5} ;$$

$$D_{K^+/q}(z_h) \propto (1-z_h)^{1-\alpha_{K^*}(0)} = (1-z_h)^{0.8} . \quad (44)$$

Since the induced energy loss leads to a shift in $z_h \Rightarrow z_h + \Delta z_h$, it should lead to a stronger suppression kaons which have a steeper fragmentation function. This expectation is in variance with HERES data depicted in Fig. 11.
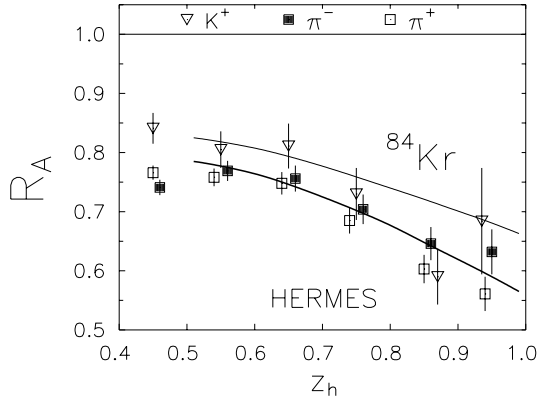

Fig. 11. Nuclear ratios for pions (*thick curve*) and positive kaons (*thin curve*) as function of z_h predicted by our model in comparison with HERMES data

At the same time, the data agree well with our predictions shown by thick and thin curves for pions and positive kaons respectively. This fact confirms our claim that the disagreement with data for kaons seen in Fig. 10 is due to presence of small-z_h events in the data.
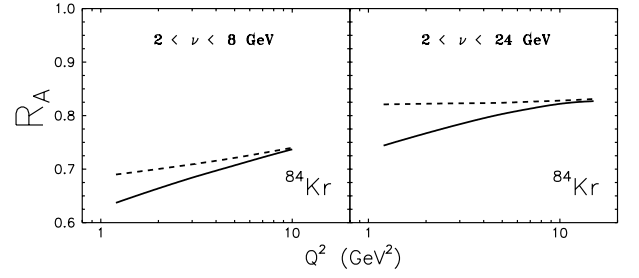

Fig. 12. The same as in Fig. 8, but predicted for krypton

Note that maximum effect of flavor dependence should be expected for shortest l_p, e.g. at $z_h \to 1$. Indeed, our calculations predict quite a large difference between nuclear effects for K^+ and pions at $z_h \to 1$, as is demonstrated in Fig. 11. Unfortunately, the accuracy of the data is not sufficient to see such a variation of the flavor dependence with z_h.

9.2 Q^2-dependence

The fit to HERMES data performed in [11] within the energy loss scenario led to the value of the universal parameter, twist-4 quark-gluon correlation tensor, which is twice as small as extracted from Drell-Yan data and 25 times smaller that follows from data on high-p_T dijet production. Such a steep variation of the parameter which must be process-independent was attributed in [11] to a strong scale dependence. If it were true, the induced energy loss effect would rise with Q^2. Accordingly, the nuclear suppression should become stronger at larger Q^2. This expectation is in obvious contradiction with the HERMES results depicted in Fig. 8.

On the other hand, we expect a more pronounced rise of nuclear ratio with Q^2 for heavy nuclei. Our predictions for krypton are depicted in Fig. 12. Note the sizeable variation of nuclear suppression with Q^2 at low energies. In this case the production time is short at any Q^2 and the variation of nuclear effects versus Q^2 is only due to color transparency. This is why the nuclear ratio steeply rises with Q^2.

9.3 z_h dependence of p_T-broadening

According to discussion in the previous section, nuclear broadening of the transverse momentum distribution might be a most sensitive probe for the production length, and provides a direct measurement of l_p, since $\Delta p_T^2 \propto l_p$. Indeed, only the hadronizing quark at short time interval $t < t_p$ contributes to the broadening. As far as the pre-hadron is created, no further broadening occurs, since inelastic interactions are prohibited for the pre-hadron, and only broadening via elastic rescattering are possible. However, the elastic cross section is so small that even for pions the mean free path in nuclear matter is about 20 fm. It is even longer for a small-size pre-hadron due to
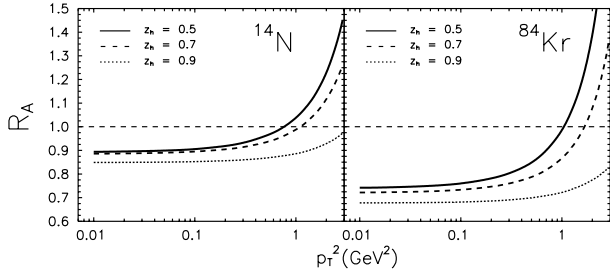
Fig. 13. p_T-dependence of nucleus-to-nucleon ratios binned in z_h for hadroproduction in DIS on nitrogen (*left*) and krypton (*right*)

color transparency. Therefore, we should expect a disappearance of the broadening effect at large $z_h \to 1$ since $t_p \to 0$. In Fig. 13 we show our predictions for the nuclear ratio as function of p_T for different z_h bins.

Note, however, that broadening should be weaker at larger z_h for any model which is able to describe the observed z_h-dependence of the nuclear ratio (see Fig. 7). Indeed, the fact that $R_A(z_h) < 1$ implies that DIS happens only in a part of the nuclear volume, namely its back side. Then, the fact that $R_A(z_h)$ decreases towards $z_h = 1$ means that a smaller part of the nuclear volume is working at larger z_h, i.e. the DIS reaction is pushed towards the back surface of the nucleus. Therefore, even in the energy loss model the path available for broadening (from the DIS point and on) becomes shorter at large z_h. This should also lead to a reduction of the broadening, but rather small, only about 10% for nitrogen and 20% for krypton. At the same time, in our approach the broadening completely vanishes at $z_h \to 1$ since $l_p \to 0$. It would be extremely important for HERMES and the experiment running at Jefferson Lab [47] to provide relevant data.

9.4 Double hadron production

One may think that a process of double hadron production is a sensitive tool which is able to disentangle the inside-outside hadronization. If absorption of the pre-hadrons is the main contributer to nuclear suppression, naively one would expect the nuclear ratio for double-hadron production to be squared, i.e. quite less, compared to inclusive single-hadron channel.

A closer look, however, shows that the situation is quite complicated and such an expectation is oversimplified. Let us assume that the two pre-hadrons are created inside the nuclear medium with production lengths l_1 and l_2 respectively, and $l_2 > l_1$. For the sake of simplicity, just for this consideration, we assume that the nuclear density is constant, both hadrons have the same and constant absorption cross sections σ, and we neglect any additional suppression related to induced energy loss. Then it is straightforward to write the nuclear suppression ratio at given impact parameter b,

$$R_A^{(2h)}(b) = \int\limits_{-\infty}^{\infty} dz\, \rho_A(b,z) \exp\left[-\sigma \int\limits_{z+l_1}^{\infty} dz'\, \rho_A(b,z')\right]$$
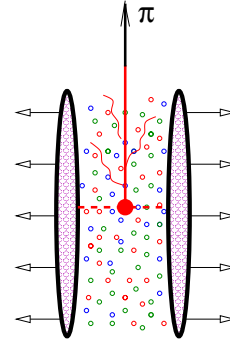

Fig. 14. Propagation and hadronization of a high-k_T parton in the dense partonic matter created right after collision of two nuclei in their c.m. frame

$$\times \exp\left[-\sigma \int\limits_{z+l_2}^{\infty} dz'\, \rho_A(b,z')\right] \tag{45}$$

Neglecting $\exp(-2\sigma\rho_A L) \ll 1$, where $L = \sqrt{R_A^2 - b^2}$, we arrive at the relative, double to single hadron production, nuclear suppressions,

$$\frac{R_A^{(2h)}(b)}{R_A^{(1h)}(b)} = \frac{1 - \frac{1}{2}\exp(-\sigma\rho_A \Delta l) + \sigma\rho_A l_1}{1 + \sigma\rho_A l_p}, \tag{46}$$

where $\Delta l = l_2 - l_1$ and l_p is the single-hadron production length. This ratio varies dependent on the values of l_1, l_2, l_p and the mean free path, $1/\sigma\rho_A$, in the medium. In the case of a very dense matter, e.g. produced in heavy ion collisions, one should expect $l\sigma\rho_A \gg 1$. Contrary to naive expectations, the production rates of single and double hadrons according to (46) should be suppressed equally. The data for high-p_T production at RHIC (see next section) seem to confirm this. This situation may change at very large p_T due to contraction of the production lengths [see (49)].

In the case of DIS in the dilute nuclear medium production lengths are comparable with the mean free path, which is about 2 fm. Then the result should vary dependent on values of z_h for each of the hadrons. For instance, if values of z_h in both cases approach their maximal values, i.e. $z_h \to 1$ and $z_{h1} + z_{h2} \to 1$, all production lengths vanish, and the ratio (46) equals 1/2, i.e. a double-hadron is suppressed twice as much as a single-hadron.

10 Heavy ion collisions: Energy loss or absorption?

Situation in the process of high-p_T hadron production in heavy ion collisions at very high energies is similar to the process of hadron production in DIS off nuclei at medium energies. Indeed the cartoon in Fig. 14 shows the development of hadronization after the nuclear disks passed through each other. Lots of partons are created from vacuum forming a dense medium of about the transverse size of the nuclei. The high-p_T parton which was created in a

hard partonic reaction at the earliest stage of nuclear collision is propagating through this medium. This process ends up with production of a hadron detected at macroscopic distances. The momenta of the hadrons in the c.m. frame of collisions ranges from a few up to 10 GeV (in the available data), what overlaps with kinematics of HERMES [2] and experiment running at Jefferson Lab [47].

Kinematics and interpretation of this process are much less certain than in DIS. In the latter case the initial quark energy is known, as well as z_h, the density and size of the medium. On the contrary, the production cross section of a high-k_T parton is a result of convolution of the initial parton distributions, hard partonic cross section, and fragmentation functions. Therefore the initial parton energy and values z_h are not known. Besides, one has to sum up over different species of partons.

These measurements are aimed at probing the density of the created medium, which is varying in space and time. This brings even more model dependence to the interpretation of data. In view of these uncertainties in interpretation of data on heavy ion collisions, one desperately needs a reliable model of in-medium hadronization tested in more certain situations like DIS.

There is a principal difference between hadronization processes in DIS and high-p_T hadron production at the mid rapidity. The dependence of the production time, l_p, on the jet energy varies substantially dependent on a process. Indeed, our previous experience says that the production time is proportional to the jet energy (the Lorentz factor). In soft interactions,

$$l_p \propto \frac{\nu}{\kappa} . \tag{47}$$

The string tension κ in the denominator provides the correct dimension for l_p.

In the case of DIS the production time is also proportional to energy, but depends on the photon virtuality,

$$l_p \propto \frac{\nu}{Q^2} . \tag{48}$$

Here the right dimension is provided by the photon virtuality, Q^2. The physics is transparent: the higher is Q^2, the stronger is the kick from the photon, the more intensive is gluon radiation and vacuum energy loss by the quark. Correspondingly, the shorter must be the color neutralization time, l_p, if one wants to produce a leading hadron with large z_h.

Now we are coming to the point. In the case of 90° parton scattering, like in the process illustrated in Fig. 14, the jet energy ($\nu \Rightarrow k_T$) and the parton virtuality ($Q^2 \Rightarrow k_T^2$) are controlled by the same parameter, which is the transverse momentum of the parton, k_T. Therefore, in this case,

$$l_p \propto \frac{1}{k_T} . \tag{49}$$

It is clear why the energy dependence of the production time switches to the inverse. The vacuum energy loss with a rate proportional to k_T^2 is so intensive, that in spite of
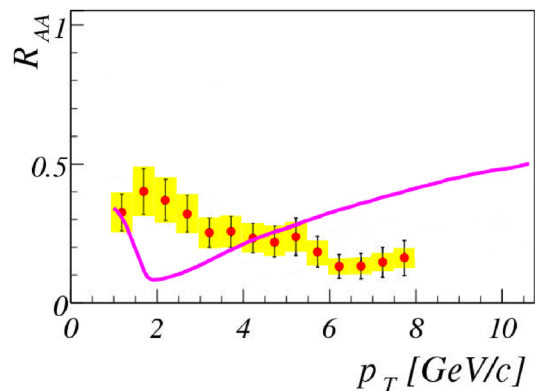

Fig. 15. Data from the PHENIX experiment [48] for pion suppression in 10% central gold-gold collisions at $\sqrt{s} = 130$ GeV in comparison with the prediction from [11]. The figure is borrowed from [48]

the Lorentz factor k_T, the hadronization process must finish shortly after the hard partonic collision, otherwise the parton energy will degrade too much, making impossible production of an energetic hadron.

It is also clear that in pure perturbative QCD calculations the dimensional parameter, Λ_{QCD}, can emerge only under a log. Therefore, (49) presents the unique possibility to provide the correct dimension for l_p. Thus, the higher is the energy of the jet, the faster the leading pre-hadron is produced. This outrageous conclusion may contradict a simple intuition based on the experience with the string model.

The energy dependence of the production length suggested by (49) for high-p_T processes is inverse to what one has for DIS, (48). Correspondingly, energy dependence of nuclear suppression should be opposite to DIS. As long as the nuclear ratio in DIS rises with energy (Figs. 5–10), we should expect a falling p_T-dependence of the nuclear ratio for heavy ion collisions. This unusual effect was indeed observed at RHIC. Data from the PHENIX experiment depicted in Fig. 15 demonstrate quite a strong fall of the ratio at $p_T > 2$ GeV. Of course at high p_T one should expect saturation ($l_p = 0$) and following rise due to color transparency.

On the contrary, in the energy loss scenario, there is no principal difference between the two cases. As long as the nuclear ratio rises with energy in DIS, it must rise with p_T in heavy ion collisions (unless one makes different models of hadronization in the two reactions). Such a behavior was indeed predicted in [11] as is shown in Fig. 15. That was a true prediction before the data at high p_T were released. Of course, once data are known, one can find explanation introducing new exotic physical assumptions.

11 Conclusions and discussion

The model of in-medium hadronization [1] developed long time ago (last century) has successfully predicted the nuclear effects for inclusive electroproduction of leading

hadrons. It was realized that the string model is rather irrelevant to the early stage of hadronization in such a perturbative QCD process as DIS. Instead, there has been developed a perturbative description which possessed a clear pattern for the space-time evolution, and allowed to do numerical estimates. The key points of the model are as follows.

– A leading quark originated from DIS loses energy for hadronization which we treat perturbatively via gluon bremsstrahlung. It is important to discriminate between *vacuum* and *induced* energy losses (which are frequently mixed up). The former is always present, even on a free nucleon target, and is the main source of energy loss. In the case of in-medium hadronization the quark radiates more gluons due to multiple soft interaction with the medium. This correction is usually much smaller than the vacuum energy loss.

– It is important to discriminate between *production* and *formation* times (which are frequently mixed up). Energy loss (both vacuum and induced) stops when a color neutralization happens, i.e. the leading quark picks up an antiquark and produces a pre-hadron, which is a colorless $\bar{q}q$ dipole with no stationary wave function. The corresponding time interval is called *production time*, or production length. Energy conservation enforces the production time to vanish at the kinematic limit of production of hadrons with maximal possible energy ($z_h \to 1$).

– The pre-hadron attenuates on its way out of the nucleus with an absorptive cross section which is controlled by the varying dipole size. Color transparency is an important ingredient of this dynamics. Eventually, on a longer time scale, called *formation time* (or length) the dipole develops the hadronic wave function. We employ a rigorous quantum-mechanical description of this process within the light-cone Green function approach. Contrary to the production length vanishing at $z_h \to 1$, the formation length reaches a maximal value in this limit.

– All these effects important for nuclear modification of the hadron production rate can be evaluated. Then the model is able to predict in a parameter free way nuclear effects in DIS as function of energy, z_h, Q^2 and p_T. Data from HERMES nicely confirm the predictions.

– Searching for observables which are able to disentangle different models, we concluded that the energy loss scenario should have problems explaining already available data for flavor and Q^2 dependence of nuclear suppression. This model is insensitive to the hadronic size, but the difference in fragmentation function at $z_h \to 1$ leads to more suppression for kaons than for pions. This is in variance with HERMES data. Also comparison of data on different reactions at different hard scales led to a conclusion that p_T broadening and energy loss rise with Q^2. Such an expectation also contradicts HERMES data. It would be very informative to have data on variation of p_T-distribution with z_h, which is a direct way to measure the production length.

– The new feature of hadronization dynamics in high-p_T processes is an inverse dependence of the production time on the jet energy compared to what is known for DIS. Correspondingly, the p_T-dependence of nuclear suppression in heavy ion collisions should be enhanced at larger p_T, contrary to DIS where nuclear effects vanish at high energy. Such a puzzling behavior was indeed disclosed by recent measurements at RHIC. Nevertheless, at higher p_T we expect the effect of color transparency to take over, then the k_T-factorization will be restored.

References

1. B.Z. Kopeliovich, J. Nemchik, and E. Predazzi: Proceedings of the workshop on Future Physics at HERA, ed. by G. Ingelman, A. De Roeck and R. Klanner, DESY 1995/1996, v. 2, 1038 (nucl-th/9607036); Proceedings of the ELFE Summer School on Confinement physics, ed. by S.D. Bass and P.A.M. Guichon, Cambridge 1995, Editions Frontieres, p. 391 (hep-ph/9511214)
2. HERMES Collaboration, A. Airapetian et al.: Eur. Phys. J. C **20**, 479 (2001) (hep-ex/0012049); V. Miccifora et al.: Nucl. Phys. A **715**, 506 (2003) (hep-ex/0106088); A. Airapetian et al.: hep-ex/0307023
3. A. Bialas: Acta Phys. Polon. B **11**, 475 (1980)
4. B.Z. Kopeliovich and F. Niedermayer: Sov. J. Nucl. Phys. **42**, 504 (1985); Yad. Fiz. **42**, 797 (1985)
5. A. Bialas and J. Czyzewski: Phys. Lett. B **222**, 132 (1989)
6. B.Z. Kopeliovich: Phys. Lett. B **243**, 141 (1990)
7. J. Czyzewski and P. Sawicki: Z. Phys. C **56**, 493 (1992)
8. A. Accardi, V. Muccifora, and H.J. Pirner: Nucl. Phys. A **720**, 131 (2003)
9. T. Falter, W. Cassing, K. Gallmeister, and U. Mosel: nucl-th/0303011
10. N.Z. Akopov, G.M. Elbakian, and L.A. Grigoryan: hep-ph/0205123
11. E. Wang and X.-N. Wang: Phys. Rev. Lett. **89**, 162301 (2002)
12. F. Arleo: Eur. Phys. J. C **30**, 213 (2003)
13. M. Gyulassy and M. Plümer: Nucl. Phys. B **346**, 1 (1989)
14. A. Casher, H. Neubereger, and S. Nussinov: Phys. Rev. D **20**, 179 (1979)
15. F. Niedermayer: Phys. Rev. D **34**, 3494 (1986)
16. S.J. Brodsky and P. Hoyer: Phys. Lett. **298B**, 165 (1993)
17. R. Baier et al.: Nucl. Phys. B **484**, 265 (1997)
18. J. Dolejsi, J. Hüfner, and B.Z. Kopeliovich: Phys. Lett. B **312**, 235 (1993)
19. M.B. Johnson, B.Z. Kopeliovich, and A.V. Tarasov: Phys. Rev. C **63**, 035203 (1991)
20. M.B. Johnson et al.: Phys. Rev. Lett. **86**, 4483 (2001); Phys. Rev. C **65**, 025203 (2002)

21. HERMES Collaboration, A. Airapetian et al.: Phys. Rev. Lett. **90**, 052501 (2003)

22. B.Z. Kopeliovich, J. Nemchik, A. Schäfer, and A.V. Tarasov: Phys. Rev. C **65**, 035201 (2002)

23. B.Z. Kopeliovich and L.I. Lapidus: in Proc. of the VI Balaton Conference on Nuclear Physics, Balatonfuered, Hungary, 1983, p. 73

24. A. Bialas and M. Gyulassy: Nucl. Phys. B **291**, 793 (1987)

25. V.T. Kim and B.Z. Kopeliovich: JINR preprint, **E2-89-727**, Dubna, 1989

26. B.Z. Kopeliovich, L.B. Litov, and J. Nemchik: J. Mod. Phys. E **4**, 767 (1993)

27. B.Z. Kopeliovich, L.I. Lapidus, and A.B. Zamolodchikov: JETP Lett. **33**, 595 (1981)

28. J. Bertch, S.J. Brodsky, A.S. Goldhaber, and J.G. Gunion: Phys. Rev. Lett. **47**, 297 (1981)

29. A. Capella et al.: Phys. Rep. **236**, 225 (1994); A.B. Kaidalov: JETP Lett. **32**, 474 (1980); Sov. J. Nucl. Phys. **33**, 733 (1981); Phys. Lett. **116B**, 459 (1982)

30. B.Z. Kopeliovich, I.K. Potashnikova, B. Povh, and E. Predazzi: Phys. Rev. Lett. **85**, 507 (2000); Phys. Rev. D **63**, 054001 (2001)

31. J.F. Gunion and G. Bertsch: Phys. Rev. D **25**, 746 (1982)

32. A.H. Mueller: Nucl. Phys. B **415**, 373 (1994)

33. B. Andersson et al.: Z. Phys. C **49**, 79 (1991)

34. S.R. Amendolia et al.: Phys. Lett. B **178**, 435 (1986)

35. J. Binnewies, B.A. Kniehl, and G. Kramer: Z. Phys. C **65**, 471 (1995)

36. B.A. Kniehl, G. Kramer, and B. Potter: Nucl. Phys. B **597**, 337 (2001)

37. B.Z. Kopeliovich and B.G. Zakharov: Phys. Rev. D **44**, 3466 (1991)

38. B.Z. Kopeliovich, A. Schäfer, and A.V. Tarasov: Phys. Rev. C **59**, 1609 (1999) (extended version in hep-ph/9808378)

39. B.Z. Kopeliovich, A. Schäfer, and A.V. Tarasov: Phys. Rev. D **62**, 054022 (2000)

40. R.P. Feynman and A.R. Gibbs: Quantum Mechanics and Path Integrals, McGRAW–HILL Book Company, New York 1965

41. B.Z. Kopeliovich, J. Raufeisen and A.V. Tarasov: Phys. Lett. B **440**, 151 (1998); Phys. Rev. C **62**, 035204 (2000)

42. EMC Collaboration, J. Ashman et al.: Z. Phys. C **52**, 1 (1991)

43. L.S. Osborne et al.: Phys. Rev. Lett. **40**, 1624 (1978)

44. N. Pavel: Ph. D. Thesis, **WUB 89-24** (1989) Wuppertal

45. HERMES Collaboration: preliminary, in http://www-hermes.desy.de/notes/pub/trans-public-subject.html#HADRON-ATTENUATION

46. J.F. Martin et al.: Phys. Rev. D **20**, 5 (1979); J.T. Dakin et al.: Phys. Rev. D **10**, 1401 (1974)

47. W. Brooks: 'Jefferson Lab experiment E02-104', talk at the 2d International Conference on Nuclear and Particle Physics by CEBAF at JLAB, May 26-31, 2003, Dubrovnic, Croatia

48. S. Mioduszewski: High-p_T measurements from Phenix, talk at Quark Matter 2002, Long Island, New York, USA (http://www.phenix.bnl.gov/conf_2002.html)

49. B.Z. Kopeliovich and J. Nemchik: JINR preprint **E2-91-150** (1991) Dubna

50. B.Z. Kopeliovich and J. Nemchik: Preprint SANITA **INFN-ISS 91/3** Rome, 1991